A Study of Ionospheric Heavy Ions in the Terrestrial Magnetotail Using ARTEMIS

Mohammad Barani[1], Andrew Reinhold Poppe[1], Matthew O. Fillingim[1], James P. Mcfadden[1], and Jasper S. Halekas[2]

[1]University of California, Berkeley
[2]University of Iowa

December 10, 2023

Abstract

Ionospheric heavy ions in the distant tail of the Earth's magnetosphere at lunar distances are observed using the ARTEMIS mission. These heavy ions are originally produced in the terrestrial ionosphere. Using the ElectroStatic Analyzers (ESA) onboard the two probes orbiting the Moon, these heavy ions are observed as cold populations with distinct energies higher than the baseline energy of protons, with the energy-per-charge values for the heavy populations highly correlated with the proton energies. We conducted a full solar cycle survey of these heavy ion observations, including the flux, location, and drift energy, as well as the correlations with the solar wind and geomagnetic indices. The likelihood of finding these heavy ions in the preferred regions of observation called "loaded" quadrants of the terrestrial magnetotail is ~90%, regardless of the z orientation of the IMF. We characterize the ratio of the heavy ion energy to the proton energy, as well as the velocity ratio of these two populations, for events from 2010 to mid-2023. This study shows that the "common velocity" assumption for the proton and heavy ion particles, as suggested in previous work through the velocity filter effect, is not necessarily valid in this case. Challenges in the identification of the mass of the heavy ions due to the ESA's lack of ion composition discrimination are addressed. It is proposed that at the lunar distances the heavy ion population mainly consists of atomic oxygen ions (O+) with velocities ~25% more than the velocity of the co-located proton population.

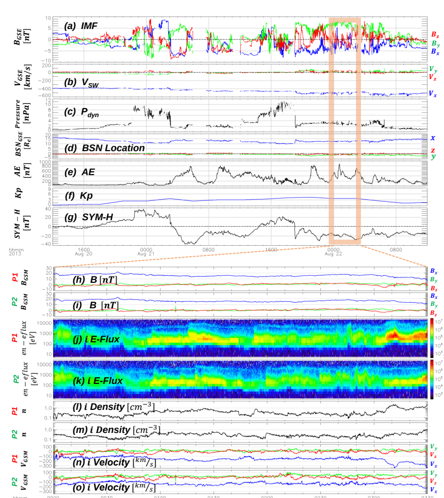

Figure 1. Solar wind and geomagnetic indices (OMNI data, panels (a) to (g)) as well as ARTEMIS P1 and ARTEMIS P2 magnetic field and ions particle data and the corresponding moments during a cold heavy ion measurement on 22 August 2013 between 00:00 and 03:30 UT. Panels (j) and (k) are differential energy flux from ElectroStatic Analyzers in which the cold heavy ion beams are noticeable as upper narrow population situated above the main proton population. Panels (l) and (m) are the ion densities, and (n) and (o) are the drift (bulk) velocity moments.

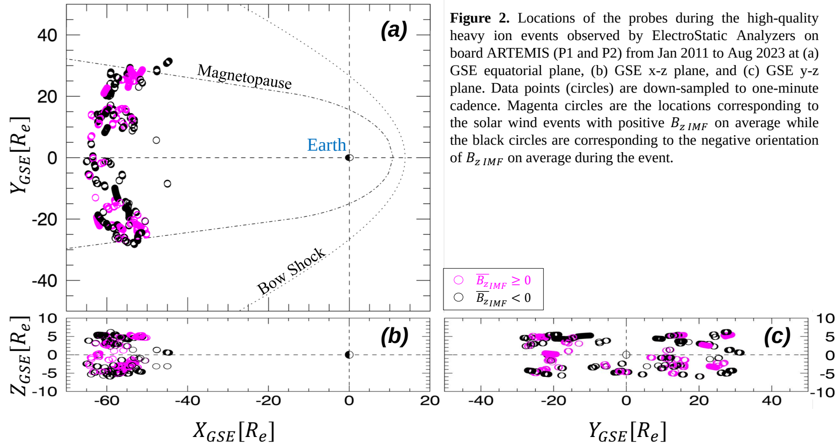

Figure 2. Locations of the probes during the high-quality heavy ion events observed by ElectroStatic Analyzers on board ARTEMIS (P1 and P2) from Jan 2011 to Aug 2023 at (a) GSE equatorial plane, (b) GSE x-z plane, and (c) GSE y-z plane. Data points (circles) are down-sampled to one-minute cadence. Magenta circles are the locations corresponding to the solar wind events with positive $B_{z\,IMF}$ on average while the black circles are corresponding to the negative orientation of $B_{z\,IMF}$ on average during the event.

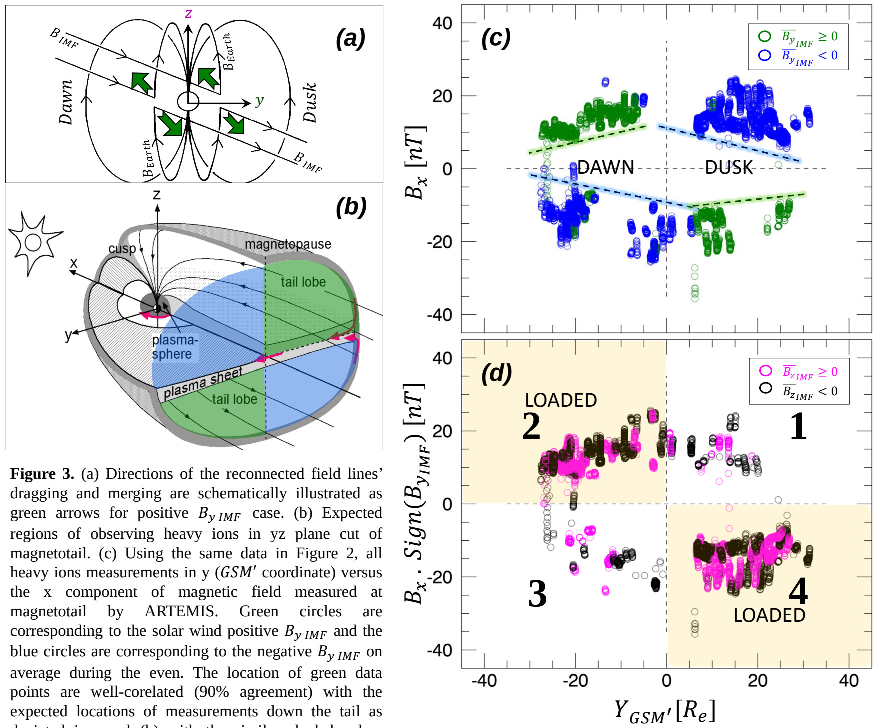

Figure 3. (a) Directions of the reconnected field lines' dragging and merging are schematically illustrated as green arrows for positive $B_{y\,IMF}$ case. (b) Expected regions of observing heavy ions in yz plane cut of magnetotail. (c) Using the same data in Figure 2, all heavy ions measurements in y (GSM' coordinate) versus the x component of magnetic field measured at magnetotail by ARTEMIS. Green circles are corresponding to the solar wind positive $B_{y\,IMF}$ and the blue circles are corresponding to the negative $B_{y\,IMF}$ on average during the even. The location of green data points are well-corelated (90% agreement) with the expected locations of measurements down the tail as depicted in panel (b) with the similar shaded colors corresponding to the same $\overline{B}_{y_{IMF}}$orientation (green is positive and blue is negative). (d) Quadrant plot for the same data. Magenta circles are corresponding to the solar wind positive $B_{z\,IMF}$ and the black circles are corresponding to the negative $B_{z\,IMF}$. The yellow-shaded regions are loaded (number 2 and 4) quadrants. Data points (circles) in (c-d) are down-sampled to one-minute cadence. IMF data are the OMNI data. The data in (c-d) are in GSM' coordinate coordinate system which is same as GSM but rotated 4 degrees dawnward to account for the aberration due to the orbital motion of the Earth with respect to the sun. In the GSM' coordinate, the OMNI data are time shifted by 40 minutes to account for the delay between arrival of the solar wind at the location of the ARTEMIS spacecraft (the lunar orbit) and the location of the magnetopause at the dayside nose of the magnetosphere. The loaded quadrants occurrence rate is more than ~90% of the total data points. Panel (a) is adapted from Gosling et al., 1985, and panel (b) is adapted from Figure 1.2 of http://urn.fi/URN:ISBN:952-91-5949-8 courtesy of Minna Palmroth.

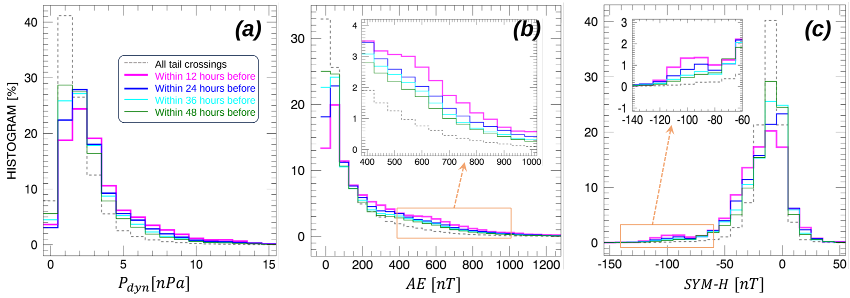

Figure 4. Histograms in % of (a) solar wind dynamic pressure, (b) Auroral Electrojet, and (c) SYM-H indices. The gray dashed lines are the occurrence during the entire times that both probes spent inside the magnetospheric tail between the two magnetopause borders (tail crossing). Magenta colors are associated with the data during the time intervals of 12 hours before until the moment the heavy ions observed at the tail. Other colors are associated with longer times until the start of observation mentioned in the legend of panel (a).

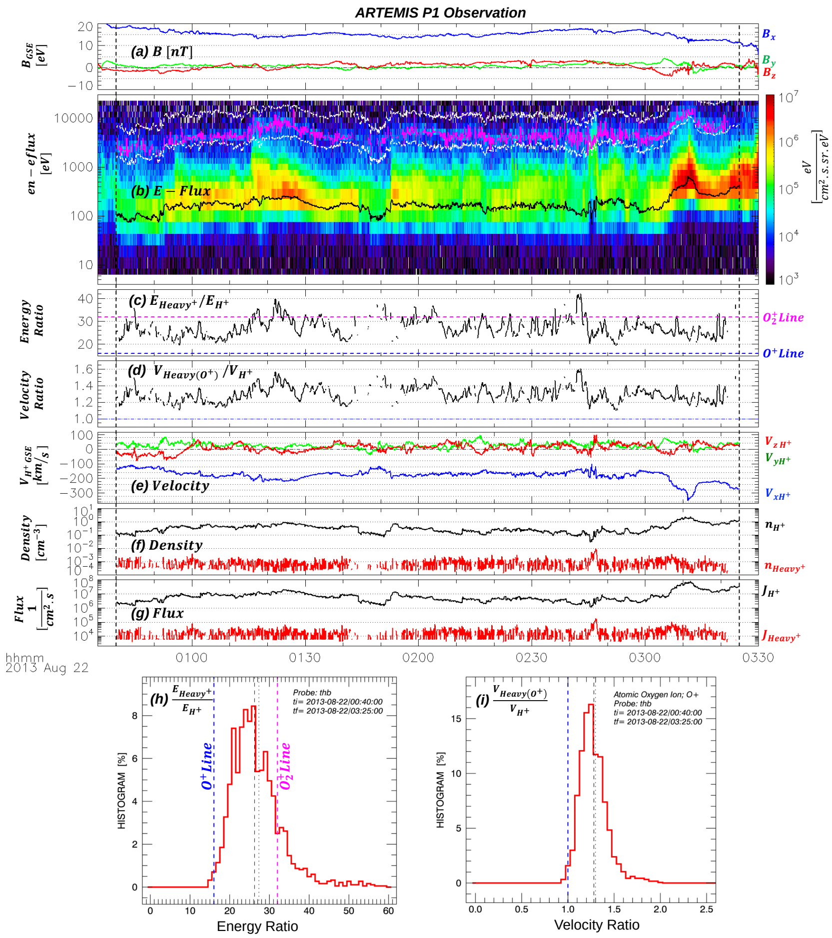

Figure 5. Magenta curve in panel (b) is E_{Heavy^+} the calculated drift energy of heavy population from the data points between the two white dashed lines while the black curve is E_{H^+} the drift energy of the proton population that calculated from the data points under the lower white dashed line. The ratio between the two calculated drift energy (running-averaged with 1 min width) is visualized in panel (c) as black curve. The blue (magenta) dashed line in (c) is the expected line if the heavy ion population contains O^+ (O_2^+) corresponding to 16 (32) assuming all species have the velocity. Panel (d) shows the calculated velocity ratio (also running-averaged with 1 min width) if the heavy ions are considered atomic oxygen O^+. Panel (e) is the proton velocities. (f) and (g) are the densities and fluxes calculated for the proton (black color) and heavy (red color) populations. (h) and (i) are histograms of the calculated energy and velocity ratios respectively. No assumption for the ions' mass is needed in (h) and no running averaging are performed for the histograms. O^+ for the heavy ions was assumed in velocity ratio calculations same as (d).

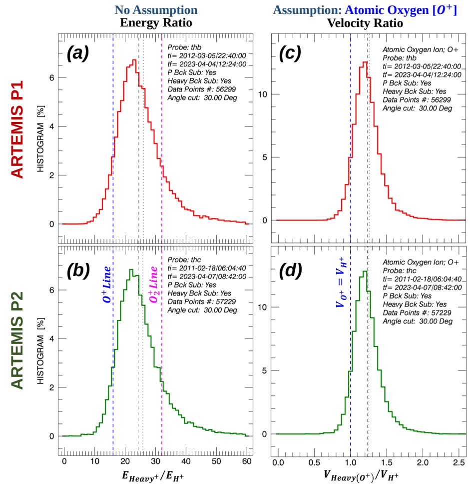

Figure 6. Histogram plots of (a) and (b) heavy ion to proton energy ratio for the entire events measured by ARTEMIS P1 (red) and ARTEMIS P2 (green) respectively, (c) and (d) atomic oxygen to proton velocity ratio for the entire events measured by ARTEMIS P1 and ARTEMIS P2 respectively. Dashed blue and dashed magenta lines in (a-b) are the expected atomic and molecular oxygen ion lines respectively if the equal-velocity assumption (with protons) is considered for the heavy ions. The dashed blue lines in (c-d) is the expected velocity if the assumed atomic oxygen ions if heavy particles happened to have exactly the same velocity as the proton population. No running average or down sampling is performed for this Figure. The locations of the measurement were already depicted in Figure 2. Dashed black and dotted black lines in all four panels are the median and mean values respectively.

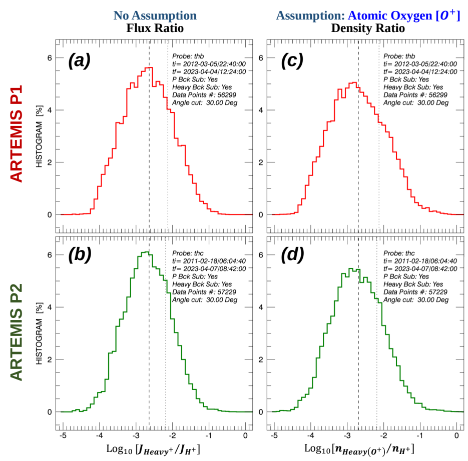

Figure 7. Histogram plots of (a) and (b) heavy ion to proton Log_{10}flux ratio for the entire events measured by ARTEMIS P1 (red) and ARTEMIS P2 (green) respectively, (c) and (d) atomic oxygen to proton Log_{10} density ratio for the entire events measured by ARTEMIS P1 (red) and ARTEMIS P2 (green) respectively. No running average or down sampling is performed for this Figure. The locations of the observation were already depicted in Figure 2. Dashed black and dotted black lines in all four panels are the median and mean values respectively.

Index	Event Occurrence (at least once)		
$P_{dyn} > 4\ nPa$	9%	71%	1%
$AE > 800\ nT$	4%	64%	8%
$SYM - H_{min}$	20%	37%	36%
$Epoch\ Time$ $[Hours]$	-24 to -12	-12 to 0	0 to 6

Table 1. Association of P_{dyn}, AE, and $SYM - H$ indices. The epoch time is mentioned at the bottom. Time 0 is the start time of observing COBs at the tail. The percentages are the fraction of events (among 86 events) in which the left column condition is satisfied at least once during the corresponding time interval. For example, during the 12 hours period before observing heavy ions, we see that in 71% of the events P_{dyn} was observed to be at least once above 4 nPa. The event occurrence rates do not add up to 100% since, for instance, for P_{dyn} case 19% of the events either have no associated intervals with $P_{dyn} > 4\ nPa$ periods or the P_{dyn} above 4 nPa happened at longer times before the observations.